Harmonic phase angle as a concentration-independent measure of nanoparticle dynamics

Adam M. Rauwerdink
Thayer School of Engineering, Dartmouth College, 8000 Cummings Hall, Hanover, New Hampshire 03755

John B. Weaver[a)]
Department of Radiology, Dartmouth-Hitchcock Medical Center, Lebanon, New Hampshire 03756 and Thayer School of Engineering, Dartmouth College, 8000 Cummings Hall, Hanover, New Hampshite 03755

(Received 28 January 2010; revised 25 March 2010; accepted for publication 14 April 2010; published 13 May 2010)

Purpose: The harmonic spectrum of magnetic nanoparticles contains valuable information about the quantity and environment of the particles. Harmonic amplitudes have been used to produce quantitative images and ratios of these amplitudes have been used to monitor changes in the particle environment. Harmonic phase angles have not yet been utilized in these pursuits. The authors explore harmonic phase angle as a concentration-independent means of remotely monitoring the dynamic magnetization of nanoparticles.
Methods: A magnetic nanoparticle spectrometer was used to explore the impacts of viscosity and excitation frequency and amplitude on the phase angle of magnetization harmonics. A dynamic model, which accounts for particle relaxation times, was used to model some results.
Results: Harmonic phase angle can undergo large changes when a nanoparticle's Brownian motion is altered. Excitation parameters and particle characteristics have a profound effect on the extent of these changes.
Conclusions: Phase angle can allow for monitoring of various impacts on a nanoparticle's Brownian motion. When combined with other concentration-independent metrics, such as ratios of harmonic amplitudes, valuable information about the particle's environment can be gathered. [DOI: 10.1118/1.3426294]

Key words: magnetic nanoparticle spectroscopy, magnetization harmonics, relaxation times, phase angle

I. INTRODUCTION

The physical properties of magnetic nanoparticles have been exploited for applications across the clinical spectrum.[1,2] Proposed applications have used both the static magnetic properties, such as magnetic targeting of aerosols,[3] and the dynamic properties. Much of the promise with magnetic nanoparticles is due to their nanometer scale, which allows them to interact with the body on a cellular or even molecular level. On the cellular level, nanoparticles can be optimized for uptake into the cells[4,5] or as a vehicle for controlling cellular functions.[6] Functionalization of the particle surface with biocompatible or biologically active coatings gives them vast clinical potential.[7]

The dynamic properties of magnetic nanoparticles have been the focus of much research, primarily *in vitro*. An applied oscillating magnetic field, or set of fields, can produce a nonlinear particle magnetization. This magnetization will contain power at higher harmonics which can be used to quantify nanoparticle concentration in magnetic immunoassays.[8,9] Environmental changes will alter the Brownian motion of the nanoparticles. The impact of these changes on the particle's magnetization can be monitored using various dynamic magnetization measurement techniques. After removal of an applied static field, thermal energy will randomize the alignment of the particle's magnetic moments. Binding or aggregating of the particles will alter the particle's relaxation curve allowing for detection of such processes using magnetorelaxometry.[10,11] In a similar fashion, AC susceptibility has been used to monitor these effects.[12] Such measurements have been performed *in vivo* but with limited resolution and speed.[13]

In 2005, magnetic particle imaging (MPI) was introduced as a means of producing 3D *in vivo* images of nanoparticle concentration.[14] A series of static gradient fields and alternating magnetic fields allow the harmonic signal of magnetic nanoparticles to be localized. By sweeping this region of localization through an object, *in vivo* images have been acquired in the milliseconds time frame.[15] Much of the effort since has focused on optimizing the MPI hardware, the acquisition and image reconstruction processes, and optimization of the nanoparticles. The harmonic spectrum is not limited to concentration-dependent measures though. Environmental and biological factors can have pronounced effects on the harmonic spectrum. Monitoring temperature's effect on the harmonic spectrum, through a ratio of harmonic amplitudes, has been proposed as a means of remotely quantifying nanoparticle temperature.[16,17] This technique relied on a theory-driven relation between nanoparticle temperature and the strength of the applied magnetic field. Dynamic effects such as changes in viscosity or molecular binding have

also been shown to influence a ratio of harmonics using a technique termed magnetic spectroscopy of nanoparticle Brownian motion (MSB).[18,19] Here we present harmonic phase angle as a means of pulling further information from the nanoparticle's harmonic spectrum. We focus on viscous effects and the impact of excitation parameters such as frequency and amplitude. A thorough understanding of the influence of particle interactions and environmental changes on the harmonic spectrum should allow for such processes to eventually serve as image contrast in MPI.

II. METHODS

II.A. Dynamic magnetization model

The static magnetization of superparamagnetic nanoparticles is well-described by the Langevin theory of paramagnetism.[20] When the particles are excited by an alternating magnetic field, relaxation times influence the nanoparticles' dynamic magnetization. The lack of such relaxation effects in the current MPI magnetization models is a known issue.[21] The response of a dipolar system to applied fields has been thoroughly examined elsewhere. Debye's calculation of the linear response of a dielectric to an oscillating field produced terms for the real and imaginary susceptibilities.[22] These susceptibility terms have been used to describe viscous influences on harmonic amplitudes[18] and for modeling of magnetic particle heating.[23] At field strengths common to MPI, the large magnetic moment of the iron particles produces a significantly nonlinear response even at room or body temperature. Felderhof *et al.*[24] have described a number of the approaches to solving this nonlinear problem. We shall focus on the effective field method[25,26] which Felderhof *et al.*[24] found to accurately approximate the dynamic particle magnetization.

The effective field method hails from the field of ferrohydrodynamics. The magnetization, in response to an alternating magnetic field of frequency ω and dimensionless amplitude ε, is governed by the differential equation

$$\frac{dM}{dt} = -\frac{1}{\tau}\left[M(t) - \frac{M(t)}{\varepsilon_E(t)}\varepsilon\cos(\omega t)\right]. \tag{1}$$

The magnetization M is calculated from the Langevin formula

$$M = L(\varepsilon) = \coth\varepsilon - \frac{1}{\varepsilon}, \quad \varepsilon = \frac{\mu H}{k_B T}, \tag{2}$$

where μ is the magnetic moment of the particle, H is the applied field, k_B is the Boltzmann's constant, and T is the absolute temperature. The effective field ε_E is calculated from $M(t)$ using the inverse of the Langevin. The relaxation time τ governs a particle's ability to follow changes in the applied field via the Neel and Brownian relaxation methods. Neel relaxation involves internal rotation of the particle's moment and is thus independent of solution viscosity. The Neel relaxation time is governed by

$$\tau_N = \tau_o \exp\left(\frac{KV_M}{k_B T}\right), \tag{3}$$

where τ_o is on the order of 10^{-9} s, K is the anisotropy of the magnetic core, and V_M is the magnetic core volume.[20] In Brownian relaxation the entire hydrodynamic volume V_H of the particle rotates according to

$$\tau_B = \frac{3\eta V_H}{k_B T}, \tag{4}$$

where η is the dynamic viscosity.

By Faraday's law of induction the voltage induced in the receive coils, our signal, is proportional to the time derivative of the particle magnetization. This induced signal will contain a series of odd harmonics of the excitation frequency. In the presence of a static field, the signal will also contain even harmonics.[27]

II.B. Spectrometer hardware

A magnetic particle spectrometer described previously was used in this study.[27] The signal was analyzed using a Stanford Research Systems (Sunnyvale, CA) SR830 lock-in amplifier. The complex third and fifth harmonics of the particles' magnetization were recorded. A small AC coil of known magnetic moment was used as a sample to calibrate our spectrometer measurements. The reference phase of the alternating drive field, produced by a resonant drive coil, has a pronounced frequency dependence. Thus, in order to generate smooth curves of higher harmonic phase versus frequency, a normalization to the first harmonic phase was needed. An important feature of such a correction is the relation between a phase shift at the fundamental frequency and a shift at the higher harmonics. As can be verified mathematically, a phase shift in the drive field will produce a threefold change in the third harmonic phase, and a fivefold change in the fifth harmonic phase.

II.C. Particles

Magnetite nanoparticles (Ocean Nanotech SHP-40, Springdale, AR) with a core size of 40 nm were used for most experiments. A Malvern (Worcestershire, UK) Zetasizer Nano ZS was used to measure the hydrodynamic size and distribution of the particles. Particle solutions with viscosities in the range of 0.96–9.81 cP were created by mixing 20 μL of the nanoparticle stock solution (100 μg Fe) in different proportions of glycerol and water. The viscosity of each solution was calculated using the equations of Cheng.[28]

III. RESULTS

For particles aligning with an external field via Brownian motion, viscosity will impact the particles' rotation and magnetization and thereby the harmonic spectrum.[18] As seen in Fig. 1, an increase in viscosity causes the magnitude of the third harmonic to decrease. Viscosity also shows a pronounced effect on the rate at which harmonic magnitudes decay with increasing harmonic number. Particle size, both

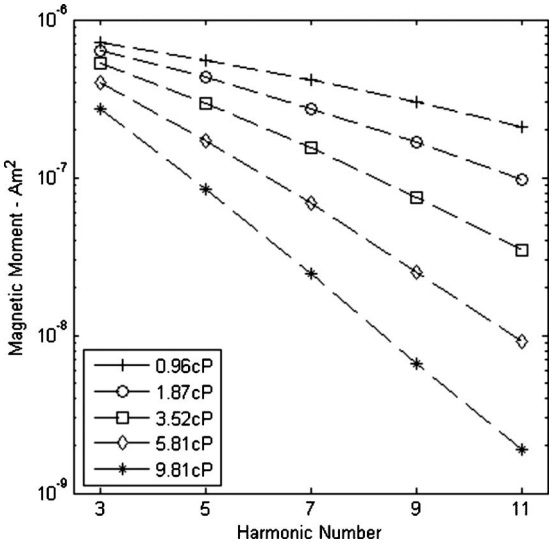

FIG. 1. The impact of viscosity on harmonic amplitudes. Field strength and frequency were 26 mT/μ_0 and 1216 Hz, respectively.

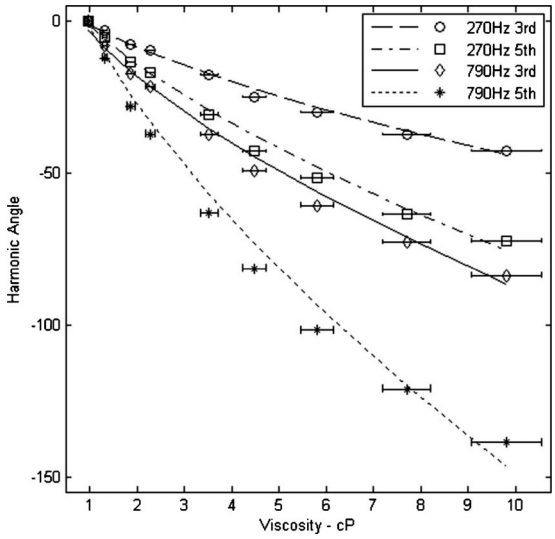

FIG. 2. The measured and calculated phase angles of the third and fifth harmonics as a function of viscosity. Data points are experimental values for third and fifth harmonic phase acquired at 270 and 790 Hz with a field strength of 26 mT/μ_0. The lines represent simulations results from Eqs. (1)–(4). A description of error bars is included in the text.

core and hydrodynamic, has a profound influence on the extent of these dynamic effects. Along with particle size and viscosity, the anisotropy of the magnetic material will determine the Shliomis diameter where Brownian and Neel relaxation have equal time constants. For magnetite based particles, such as used here, this critical magnetic core diameter is around 20 nm, though as demonstrated in Ref. 29, this value is sensitive to anisotropy. The Neel time constant increases exponentially with the cube of diameter, so for our 40 nm core particles, Brownian relaxation will dominate. A frequency of 1216 Hz was used for acquiring the data in Fig. 1. Similar measurements in the 2–3 kHz range showed increasingly rapid decay of higher harmonics. Biederer *et al.*[21] performed spectroscopic measurements on 4 nm particles, measured by TEM, at the common MPI imaging frequency of 25 kHz and showed significant higher harmonic signal. For isolated 4 nm iron-oxide cores, Neel relaxation will dominate and viscosity should not influence the signal.

Zetasizer measurements indicated a mean hydrodynamic diameter of 54.3 nm and a standard deviation of 15 nm. Assuming a 40 nm magnetic core, the measured hydrodynamic diameter indicates an average particle coating of 7.2 nm. A particle size distribution was calculated with these values using a log-normal distribution and a constant coating thickness.[18,21] Experimentally, we acquired the phase angle of the third and fifth harmonics for nine different solution viscosities at drive frequencies of 270 and 790 Hz using a field strength of 26 mT/μ_0, see Fig. 2. We simulated these same conditions using Eqs. (1)–(4). The drive frequency was the only simulation variable changed for the two separate calculations. All results were normalized to a phase angle of zero for the lowest viscosity sample.

The spectrometer phase variability with repeat measurements was approximately 0.1° at 1 cP and 1.1° at 10 cP. The larger variability results when the smaller signal at high viscosity approaches the noise floor. Another source of error is the viscosity of each sample. Temperature and percent glycerol can significantly influence the viscosity of the solution especially as the percent glycerol increases. Horizontal error bars were included in Fig. 2 to demonstrate the error associated with ±1 K accuracy in temperature and ±1% accuracy in glycerol volume. For visual clarity, the small vertical errors were not included in the figures.

For static measurements of superparamagnetic particles, a balance of thermal and magnetic energy determines the equilibrium magnetization. In the dynamic case, the particles' ability to reach this equilibrium magnetization is governed in part by the relaxation times of the particles. Thermal, magnetic, and viscous forces will influence the particles' ability to undergo Brownian motion in response to changes in the applied field. The effects of viscosity and field strength are shown in Fig. 3 at a frequency of 270 Hz. The well-described effect of field strength on the amplitude of the harmonics is seen, but an increase in field strength is also seen to dampen the effect of viscosity on phase angle. This relationship between field strength and viscosity can be discerned from Eq. (1). The sinusoidal drive field ε is continually attempting to pull the magnetic moments of the particles to an equilibrium magnetization defined by the Langevin equation. The time constant τ in Eq. (1) contains a viscosity term, as described in Eq. (4), which will govern a particle's ability to follow changes in the drive field. If unable to stay in absolute equilibrium with the drive field, a phase lag will develop between the particle and the drive field. This phase lag can be monitored via the harmonic phase angles. For the particle size and frequency presented in Fig. 3, the harder the particle was pulled, by increasing the field strength, dampened the ability of viscosity to produce a phase lag.

With field strength held constant, excitation frequency will also impact the phase angle of the harmonics. Figure 4

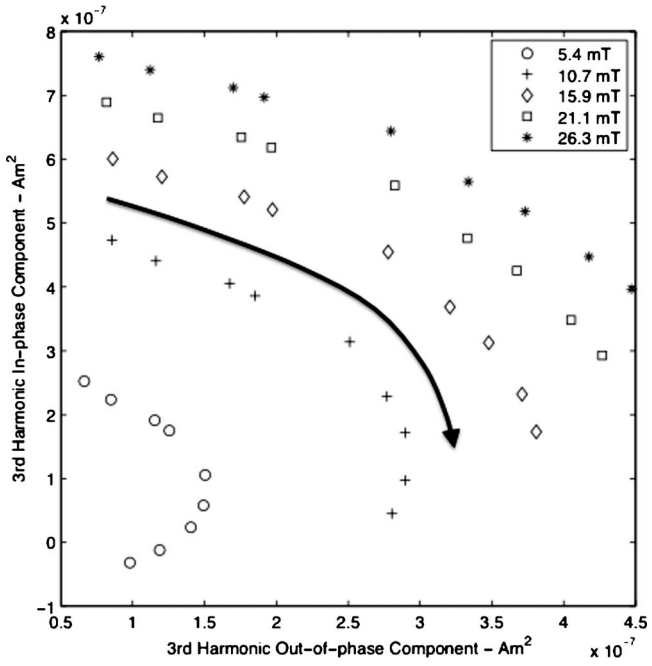

FIG. 3. In-phase and out-of-phase components of the third harmonic signal as a function of viscosity at 270 Hz. For each field amplitude, the measured data points correspond to the response at different viscosities in the range 0.96–9.81 cP. The arrow indicates the direction of increasing viscosity.

demonstrates the impact of frequency on the change in third harmonic angle with viscosity at constant field strength of 15 mT/μ_0. The impact of frequency on the sensitivity of the third harmonic angle to changes in viscosity was emphasized by normalizing the angle of the 0.96 cP sample to zero at all frequencies. Without such normalization, increases in frequency between 270 and 1740 Hz produce a monotonic 60° drop in the 0.96 cP sample's third harmonic angle. Frequency and viscosity are seen to have a similar effect on phase angle. This similarity also holds for the amplitude of the harmonics. Figure 1 showed a decrease in harmonic amplitude with viscosity. The Langevin equation would predict a linear increase in harmonic amplitude with frequency, which can be seen for particles with small relaxation times. The particles measured here failed to follow this linear increase, and instead a steady decrease in harmonic amplitude per period of the excitation field was measured.

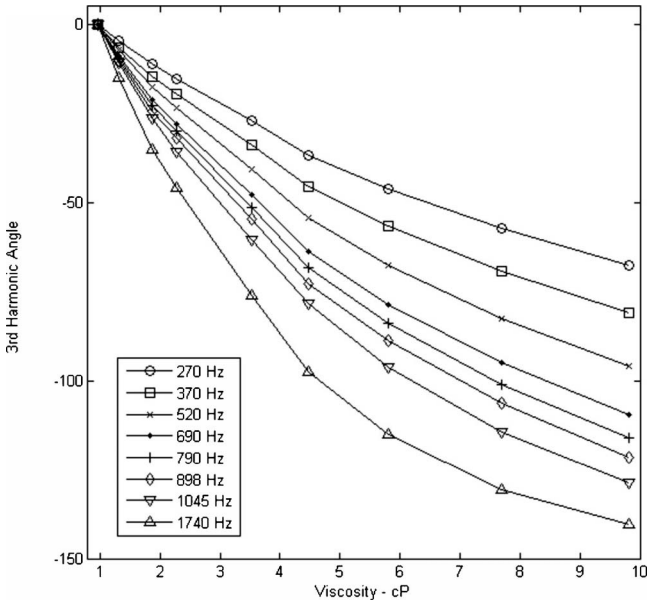

FIG. 4. Comparison of the relative change in third harmonic angle with viscosity at several frequencies. Field amplitude was held constant at 15 mT/μ_0. To emphasize the increase in phase lag across the viscosity range, measurements at each frequency were normalized to the third harmonic angle of the 0.96 cP sample.

TABLE I. Impact of different nanoparticle environments on the harmonic spectrum.

	Particle environments		
	Viscosity 0.96 cP	Viscosity 3.67 cP	Aggregated
Third harmonic angle	62.4°	27.0°	40.8°
Fifth harmonic angle	40.9°	−19.9°	−19.9°
Ratio of fifth/third amplitudes	0.705	0.433	0.191

The previous figures have demonstrated the impact particle environment can have on phase angle. The ability to use phase angle and other concentration-independent metrics to remotely determine the environment of a particle will in part depend on the extent to which these environments have a unique spectral signature. In Table I, we detail the impact of several different particle environments on harmonic phases and ratio. To acquire these data, 120 nm hydrodynamic diameter particles, coated in biocompatible dextran and containing a multicrystal core, were dispersed in a series of glycerol solutions as was done in the earlier parts of this paper with the smaller particles. A separate particle sample was mixed with the protein Concanavalin-A which cross-links dextran and causes visible aggregation of the nanoparticles. The harmonic spectra resulting from these different particle environments were acquired at 790 Hz and 26 mT/μ_0 (see Table I). A polynomial fit to a plot of fifth harmonic angle versus viscosity was used to find a solution viscosity which would produce a fifth harmonic angle comparable to that of the aggregated sample. At this calculated viscosity of approximately 3.7 cP, the third harmonic angle and the ratio of the fifth and third harmonic magnitudes are far different than those caused by aggregation.

IV. DISCUSSION

Presentation and defense of an exact numerical simulation for our experimental results is beyond the scope and intentions of this manuscript. The calculation of exact numerical solutions to the nonlinear AC response of magnetic particles is a challenging problem which has seen much investigation in the physics literature over the last few decades. We chose an approximate method to model our results as it is has been shown to quite accurately describe the magnetization[24] and its simpler form, as compared to potentially more exact solutions, allows for an easier description of the various influ-

ences on particle magnetization. Exact solutions for the case of strong AC magnetic fields, $\varepsilon \geq 1$, as are present in MPI have seen recent progress.[30]

Fitting of dynamic magnetization simulations to experimental data requires the use of several additional variables not required for static models. Static models require a log-normal size distribution of the particle core size. Dynamic models will also require a hydrodynamic size distribution. We chose a constant coating size for the results of Fig. 2 which makes variation in core size responsible for all changes in hydrodynamic size. A more accurate simulation of the particles might involve a double distribution of core and hydrodynamic sizes. Phase changes with hydrodynamic or magnetic core size necessitate complex addition of the harmonics for different sizes in a particle distribution. It is possible that different particle sizes within a distribution, if sufficiently different in phase, could oppose each other and lower the overall harmonic amplitude. The use of dynamic models to describe nanoparticle magnetization should remove some of the current limitations known to exist with the Langevin model as applied to MPI.[21] The role of particle interactions, aggregates, particle shape, and anisotropy also should be explored and applied to MPI particle models. A complete understanding of all of these effects should help guide the design of optimal nanoparticles for MPI or MSB.

The experimental results presented here were all acquired at frequencies one to two orders of magnitude lower than those currently used in MPI. The excitation parameters of field strength and frequency along with the physical characteristics of the nanoparticles will determine the extent to which environmental changes modify the harmonic spectrum. Very small particles can have Neel time constants many orders of magnitude shorter than their Brownian relaxation times. These particles will follow an alternating field via internal rotations of their moments and thus the harmonic spectrum will be independent of solution viscosity or binding. For our work, termed MSB, environmental impacts on the harmonic spectrum are the source of contrast. In MPI, where concentration is currently the source of contrast, particle and excitation parameters can be chosen which limit environmental effects. The use of higher anisotropy magnetic material could allow for smaller Brownian particles. This is turn would decrease the Brownian relaxation time and potentially allow for increased excitation frequency. Figures 3 and 4 demonstrate how excitation parameters can accentuate or dampen the impact of viscosity on harmonic phase angle. These same parameters will also impact the amplitudes of the harmonics and the rate of signal decay with increasing harmonic number. To achieve an optimal contrast to noise ratio, proper particle and excitation parameters would need to be chosen in order to balance the influence dynamic effects have on harmonic magnitudes with the impacts on harmonic phase.

Table I demonstrates the unique impact several different particle environments have on the harmonic spectrum. By using a variety of concentration-independent metrics, both the shape and phase of the harmonic magnetization can be monitored. Table I suggests that different particle interactions may result in a unique spectral signature. *In vivo*, particles will be exposed to complex and changing environments as they enter regions of different viscosity, bind to targets, are endocysed by cells, or a combination of these and other influences. By recording the harmonic response at several excitation frequencies and amplitudes, one can hope to gather a data set rich in information about the particle environment. The extent to which this data can be fully understood and interpreted remains to be seen. Successful implementation *in vivo* would have numerous applications for imaging, treatment, and basic science. Current techniques for monitoring binding *in vivo* are limited;[19] such ability could allow monitoring of a targeted nanoparticle's fate and provide insight on related disease processes and physiology. The cellular uptake of nanoparticles is actively being studied, and the ability to do this real-time *in vivo* would provide valuable information for particle delivery and therapeutics.[4,5] Cellular uptake can also have an impact on treatments such as magnetic particle hyperthermia and an ability to monitor such uptake could prove beneficial. Harmonics have already been used to quantify temperature;[16,17] the ability to remotely quantify viscosity or stiffness on the nanoscale would be beneficial in the study of diseases and for improved understanding of the underlying physics.

With MRI, the development of new pulse sequences and contrast agents has produced new clinical applications for the generally fixed magnetic and electrical hardware. Though the fundamental scans of particle concentration are still being developed for MPI, future MPI "pulse sequences" should allow for the full content of the harmonic spectrum to be utilized and interpreted. Imaging at the lower frequencies used here would require longer scan times using the current techniques. Compared to 25 kHz, the field free point would take longer to cover a set trajectory, further the signal from a region of interest might need to be measured additional times to get an adequate signal to noise ratio. The success of MPI as a clinical and preclinical imaging modality will depend to a large extent on an ability to address an array of applications. Through the creative utilization of concentration-independent metrics, such as those mentioned here and others yet unexplored, MPI should be capable of generating images where nanoparticle environment and biological interactions serve as image contrast. Potential uses of MSB techniques independent of MPI may also become apparent.

V. CONCLUSION

The physical environment of a nanoparticle can have a pronounced effect on its harmonic spectrum. Phase angle, as well as other concentration-independent metrics, will change in response to various impacts on the nanoparticle's Brownian motion. Through proper selection of particle characteristics and excitation parameters the extent of these changes to the harmonic spectrum can be amplified or dampened. With a greater understanding of how the harmonic spectrum is influenced by a particle's environment, MPI and MSB should be capable of detecting these environmental changes and using them for contrast.

[a]Author to whom correspondence should be addressed. Electronic mail: john.b.weaver@hitchcock.org

[1]Q. A. Pankhurst, N. K. T. Thanh, S. K. Jones, and J. Dobson, "Progress in applications of magnetic nanoparticles in biomedicine," J. Phys. D. **42**, 224001 (2009).
[2]P. Alivisatos, "The use of nanocrystals in biological detection," Nat. Biotechnol. **22**, 47–52 (2004).
[3]P. Dames, B. Gleich, A. Flemmer, K. Hajek, N. Seidl, F. Wiekhorst, D. Eberbeck, I. Bittmann, C. Bergemann, and T. Weyh, "Targeted delivery of magnetic aerosol droplets to the lung," Nat. Nanotechnol. **2**, 495–499 (2007).
[4]B. D. Chithrani, A. A. Ghazani, and W. C. Chan, "Determining the size and shape dependence of gold nanoparticle uptake into mammalian cells," Nano Lett. **6**, 662–668 (2006).
[5]W. Jiang, B. Y. Kim, J. T. Rutka, and W. C. Chan, "Nanoparticle-mediated cellular response is size-dependent," Nat. Nanotechnol. **3**, 145–150 (2008).
[6]J. Dobson, "Remote control of cellular behaviour with magnetic nanoparticles," Nat. Nanotechnol. **3**, 139–143 (2008).
[7]C. C. Berry, "Progress in functionalization of magnetic nanoparticles for applications in biomedicine," J. Phys. D. **42**, 224003 (2009).
[8]P. I. Nikitin, P. M. Vetoshko, and T. I. Ksenevich, "New type of biosensor based on magnetic nanoparticle detection," J. Magn. Magn. Mater. **311**, 445–449 (2007).
[9]M. H. F. Meyer, H. J. Krause, M. Hartmann, P. Miethe, J. Oster, and M. Keusgen, "Francisella tularensis detection using magnetic labels and a magnetic biosensor based on frequency mixing," J. Magn. Magn. Mater. **311**, 259–263 (2007).
[10]D. Eberbeck, C. Bergemann, F. Wiekhorst, U. Steinhoff, and L. Trahms, "Quantification of specific bindings of biomolecules by magnetorelaxometry," J. Nanobiotechnology **6** (2008).
[11]D. Eberbeck, F. Wiekhorst, U. Steinhoff, and L. Trahms, "Aggregation behaviour of magnetic nanoparticle suspensions investigated by magnetorelaxometry," J. Phys.: Condens. Matter. **18**, S2829–S2846 (2006).
[12]K. Petersson, D. Ilver, C. Johansson, and A. Krozer, "Brownian motion of aggregating nanoparticles studied by photon correlation spectroscopy and measurements of dynamic magnetic properties," Anal. Chim. Acta **573–574**, 138–146 (2006).
[13]R. Jurgons, C. Seliger, A. Hilpert, L. Trahms, S. Odenbach, and C. Alexiou, "Drug loaded magnetic nanoparticles for cancer therapy," J. Phys.: Condens. Matter **18**, S2893–S2902 (2006).
[14]B. Gleich and J. Weizenecker, "Tomographic imaging using the nonlinear response of magnetic particles," Nature (London) **435**, 1214–1217 (2005).
[15]J. Weizenecker, B. Gleich, J. Rahmer, H. Dahnke, and J. Borgert, "Three-dimensional real time in vivo magnetic particle imaging," Phys. Med. Biol. **54**, L1–L10 (2009).
[16]J. B. Weaver, A. M. Rauwerdink, and E. W. Hansen, "Magnetic nanoparticle temperature estimation," Med. Phys. **36**, 1822–1829 (2009).
[17]A. M. Rauwerdink, E. W. Hansen, and J. B. Weaver, "Nanoparticle temperature estimation in combined AC and DC magnetic fields," Phys. Med. Biol. **54**, L51–L55 (2009).
[18]A. M. Rauwerdink and J. B. Weaver, "Viscous effects on nanoparticle magnetization harmonics," J. Magn. Magn. Mater. **322**, 609–613 (2010).
[19]A. M. Rauwerdink and J. B. Weaver, "Measurement of molecular binding using the Brownian motion of magnetic nanoparticle probes," Appl. Phys. Lett. **96**, 033702 (2010).
[20]B. Cullity and C. Graham, *Introduction to Magnetic Materials*, 2nd ed. (Wiley, New Jersey, 2008).
[21]S. Biederer, T. Knopp, T. F. Sattel, K. Ludtke-Buzug, B. Gleich, J. Weizenecker, J. Borgert, and T. M. Buzug, "Magnetization response spectroscopy of superparamagnetic nanoparticles for magnetic particle imaging," J. Phys. D. **42**, 205007 (2009).
[22]P. J. W. Debye, *Polar Molecules* (The Chemical Catalog Company, NY, 1929).
[23]R. Rosensweig, "Heating magnetic fluid with alternating magnetic field," J. Magn. Magn. Mater. **252**, 370–374 (2002).
[24]B. Felderhof and R. Jones, "Nonlinear response of a dipolar system with rotational diffusion to an oscillating field," J. Phys.: Condens. Matter **15**, S1363–S1378 (2003).
[25]Y. L. Raĭkher and M. I. Shliomis, "The effective field method in the orientational kinetics of magnetic fluids," Adv. Chem. Phys. **87**, 595–752 (1994).
[26]M. I. Shliomis, "Ferrohydrodynamics: Testing a third magnetization equation," Phys. Rev. E **64**, 060501(R) (2001).
[27]J. B. Weaver, A. M. Rauwerdink, C. R. Sullivan, and I. Baker, "Frequency distribution of the nanoparticle magnetization in the presence of a static as well as a harmonic magnetic field," Med. Phys. **35**, 1988–1994 (2008).
[28]N. S. Cheng, "Formula for the viscosity of a glycerol-water mixture," Ind. Eng. Chem. Res. **47**, 3285 (2008).
[29]J. Embs, S. May, C. Wagner, A. Kityk, A. Leschhorn, and M. Lücke, "Measuring the transverse magnetization of rotating ferrofluids," Phys. Rev. E **73**, 036302 (2006).
[30]P. M. Déjardin and Y. P. Kalmykov, "Relaxation of the magnetization in uniaxial single-domain ferromagnetic particles driven by a strong AC magnetic field," J. Appl. Phys. **106**, 123908 (2009).